International Journal of Applied and Natural Sciences (IJANS)
ISSN(P): 2319-4014; ISSN(E): 2319-4022
Vol. 3, Issue 2, Mar 2014, 63-80
© IASET

International Academy of Science, Engineering and Technology
Connecting Researchers; Nurturing Innovations

# INVESTIGATION ON *N*-FORMYL PIPERIDIN-4-ONES AS CORROSION INHIBITORS FOR CARBON STEEL IN ACID MEDIUM

**A. ILAMPARITHI[1], S. PONNUSWAMY[2] & A. SELVARAJ[3]**

[1,2]PG and Research, Department of Chemistry, Government Arts College (Autonomous), Coimbatore, Tamil Nadu, India

[1]Department of Chemistry, Gobi Arts and Science College, Gobichettipalayam, Tamil Nadu, India

[3]PG and Research, Department of Chemistry, CBM College, Coimbatore, Tamil Nadu, India

## ABSTRACT

The corrosion inhibition of mild steel in 1N $H_2SO_4$ and 1N HCl in the presence of *N*-formyl piperidin-4-ones was studied using gravimetric and electrochemical techniques. Results obtained show that these compounds are excellent inhibitors and inhibit better in HCl than in $H_2SO_4$. The potentiodynamic polarisation studies clearly reveal that they are mixed type inhibitors. The impedance parameters ($R_{ct}$ and $C_{dl}$) clearly indicate the adsorption of *N*-formyl piperidin-4-ones on the metal surface leading to the formation of a protective layer which grows with increasing exposure time. The adsorption of *N*-formyl derivatives on mild steel surface in both the acid media follows a Langmuir adsorption isotherm and Tempkin adsorption isotherm. The mild steel-FP complex layer formed at the metal surface was identified by infrared spectral analysis and SEM/EDS.

**KEYWORDS:** 1. Corrosion Inhibitors, 2. Mild Steel, 3. Electrochemical Impedance Spectroscopy, 4. Polarisation Curves, 5. Adsorption Isotherm, 6. *N*-Formyl Piperidin-4-One, 7. FT-IR , 8. SEM/EDS

## INTRODUCTION

Generally HCl and $H_2SO_4$ are employed in the treatment of steel and ferrous alloys in industry. The use of inhibitors containing heteroatom's like nitrogen, oxygen, and sulphur is one of the most practical methods for protection against corrosion in acid media [1]. The aim of this study is to investigate the inhibitive properties of some azacyclic inhibitors *viz.* *N*-formyl-*t*-3-methyl-*r*-2,*c*-6-diphenylpiperidin-4-one (F3MPO), *N*-formyl-*t*-3-isopropyl-*r*-2, *c*-6-diphenylpiperidin-4-one (F3IPPO), *N*-formyl *c-3,t*-3-dimethyl-*r*-2,*c*-6-diphenylpiperidin-4-one (F3DMPO) and *N*-formyl *t*-3,*c*-5-dimethyl-*r*-2,*c*-6-diphenylpiperidin-4-one (FDMPO) on the corrosion of mild steel in sulphuric acid and hydrochloric acid. The chemical structures of the inhibitors are given in Figure 1.

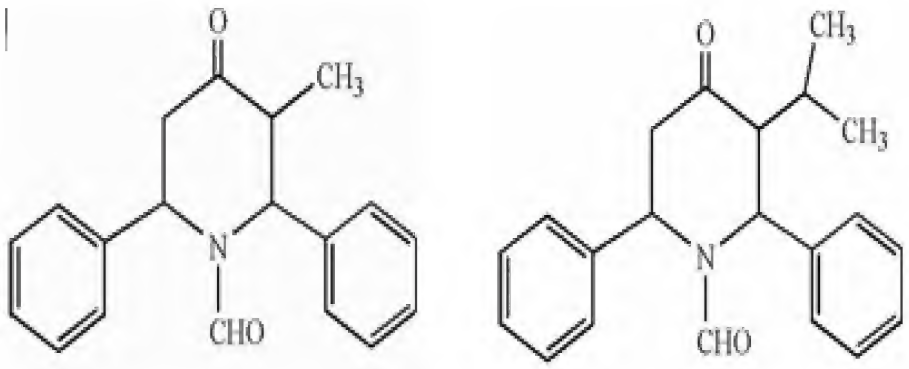


**(A)** **(B)**

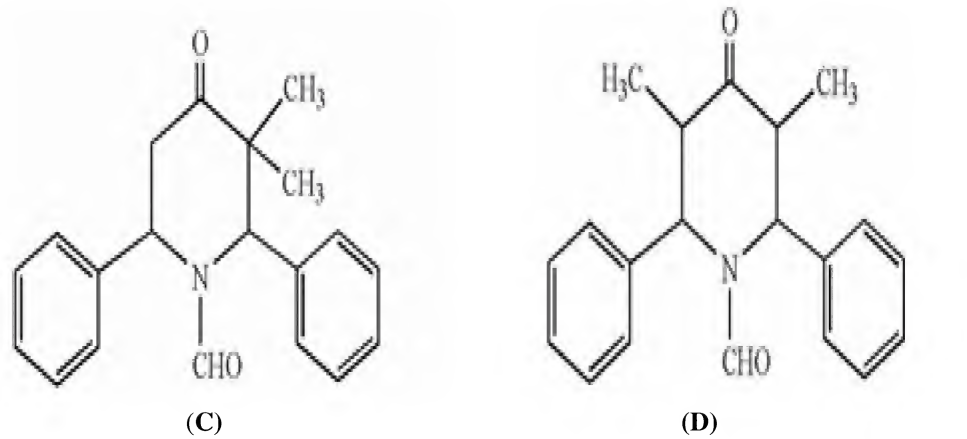


(C) (D)

**Figure 1: Structure of Inhibitors (A) F3MPO (B) F3IPPO (C) F3DMPO (D) FDMPO**

## EXPERIMENTAL

### Weight Loss Measurements

Mild steel specimens containing 0.0224% C, 0.025% Si, 0.320% Mn, 0.023% P, 0.052% S, 0.108% Ni, 0.069% Cr, 0.012% Mo, 0.047% Al, 0.011% Cu the remainder being Fe of the dimension 2.5cm×1cm×0.1cm were polished to a mirror finish using 200, 400, 600, and 800 grade emery papers and degreased with trichloroethylene and used for weight loss measurements. *N*-formyl piperidin-4-ones were synthesized as reported in literature [2-10]. Three mild steel strips were immersed in 100 ml of inhibited and uninhibited solution of 1N HCl and 1N $H_2SO_4$ for 3 h and their inhibition efficiency were determined. The efficiency was also studied at various elevated temperatures up to 323K and the weight loss measurements were also made at various time of immersion up to 24h. The corrosion rate (mm/Y), surface coverage [θ] and inhibition efficiency were calculated from the difference in weight loss values. Since the solubility of inhibitor is less and in order to avoid precipitation, 40 ml ethyl alcohol was added, to make up the solution, for all gravimetric and electrochemical studies.

### Electrochemical Analysis

For electrochemical measurements, the cell used was a conventional three-electrode Pyrex glass cell with a platinum counter electrode and a saturated calomel electrode (SCE) as reference. The working steel rod electrode was embedded in Teflon so that it's cross sectional area (1 $cm^2$) was in contact with the solution. The potentiodynamic current – potential curves were recorded by changing the electrode potential automatically from -200 to +200 mV with respect to OCP and at the scan rate of 1mV $s^{-1}$. Electrochemical impedance spectra (EIS) were carried out at $E_{corr}$ by using a Potentiostat/ Galvanostat/ FRA2 (μ Autolab type 3). Data were collected and analysed by Ivium software. The EIS data were acquired in the frequency range of 100 kHz to 1Hz with a 10 mV amplitude sine wave generated by a frequency response analyzer.

## RESULTS AND DISCUSSIONS

### Weight Loss Measurements

Table 1 gives the values of the inhibition efficiency obtained from the weight loss measurements of mild steel for different concentration of F3MPO, F3IPPO, F3DMPO and FDMPO in 1N HCl and 1N $H_2SO_4$ at $30^o$ C after 3 h immersion. F3MPO, F3IPPO, F3DMPO and FDMPO inhibit the corrosion of mild steel in an identical manner. In both the media, the inhibition efficiency increases with the increasing inhibitor concentration in the experimental condition.

The inhibition is estimated to be superior in HCl than in $H_2SO_4$ [11] and the optimum concentration required to achieve maximum efficiency was found to be 5 mM. F3IPPO is the best inhibitor and the efficiency decreases in the order F3IPPO>F3MPO>F3DMPO>FDMPO, in both the media. The same order was proposed by Sankarapapavinasam *et al.*[12] for the change of alkyl substituents of the parent piperidine-4-ones. It is apparent that the inhibition efficiency increases with increase in inhibitor concentration. It may be due to the fact that the extent of adsorption increases with the increase in concentration of the inhibitor leading to increased inhibition efficiency [13]. Perusal of Table 2 indicates that the IE(%) increases with the increase in immersion time from 1 to 12 h and remains constant thereafter. The available active sites on the metal surface seem to be covered by the inhibitor molecules completely in 12 h and thereafter rate of adsorption and desorption is same and hence the inhibiting efficiency remains constant [14].

**Effect of Addition of 1 mM Anions on the Corrosion Inhibition of MS in $H_2SO_4$**

In order to understand the synergistic and antagonistic effect of anions on the corrosion inhibition efficiency of the inhibitors, the following 1 mM anions *viz.* KCl, KBr, KI, $KNO_3$, $KBrO_3$, and KCNS were added and their efficiency was determined and shown in Table 3. The $NO_3^-$ ion and $CNS^-$ ion have poor synergetic effect and the synergistic effect increases in the order $Cl^-<Br^-<I^-$ as reported in the literature [15].

Effect of halide ions on the enhancing corrosion inhibition has also been studied by Hackermann *et al.* [16] who suggested that halide ions in general and especially iodide ion affect the steel dissolution by strong chemisorption on the metal surface and renders the surface more negatively charged. On the highly negatively charged metal surface the protonated cationic inhibitor molecules are adsorbed due to the electrostatic interaction. The interaction will be higher for $I^-$ than for $Cl^-$ or $Br^-$ due to higher magnitude of negative charge on the metal surface. Hence the observed order is $Cl^-<Br^-<I^-$.

**Effect of Temperature**

To calculate the thermodynamic parameters ($E_a$, $\Delta H^{\#}$ and $\Delta S^{\#}$) of the corrosion process and to investigate the mechanism of the inhibition process, the weight loss measurements were recorded at various temperatures (303 K to 323 K). The data obtained for the effect of temperature on the corrosion inhibition of mild steel in 1N $H_2SO_4$ in presence and absence of various inhibitors are presented in Table 4. It has been found that the weight loss and the IE (%) have increased linearly with the increase of temperature in the absence and presence of inhibitors upto 323 K.

The data obtained from weight loss measurements were plotted in accordance to Arrhenius Equation and shown in Figure 2.

$$\ln \text{rate} = (-E_a / RT) + \text{Constant} \quad (1)$$

Where $E_a$ = activation energy; R = gas constant and T= absolute temperature. The activation energies for the corrosion process are estimated from the slopes of the lines of the Arrhenius plot and given in Table 5. The values of $E_a$ for the inhibited systems were slightly lower than those of the uninhibited system.

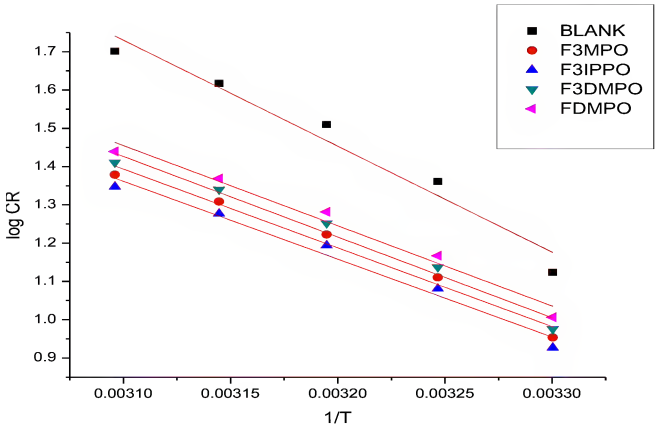


**Figure 2: The Arrhenius Plots of MS Corrosion in 1N $H_2SO_4$ Solution Containing Inhibitors**

The thermodynamic functions viz standard free energy of adsorption $\Delta G^o$, enthalpy of adsorption $\Delta H^\#$ and entropy of adsorption $\Delta S^\#$ are estimated from the transition state plot (Figure 3) and the results are given in Table 5, 6. The negative value of $\Delta G^o$ indicates strong interaction of inhibitor molecule and spontaneous adsorption of inhibitor on the surface of the mild stee l[17]. The raise in efficiency (IE%) with increase in temperature and invariance of inhibitor efficiency with immersion time beyond 12 h indicates chemisorption.

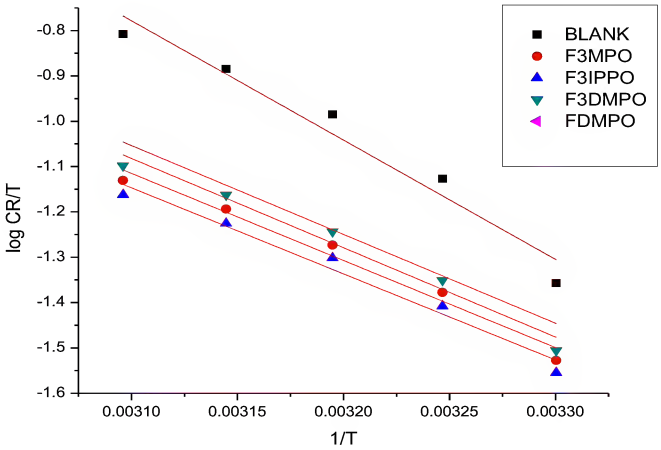


**Figure 3: The Transition State Plot of MS Corrosion in 1N $H_2SO_4$ Solution Containing Inhibitors**

**The Electrochemical Impedance Spectroscopy**

The corrosion behaviour of mild steel in 1N $H_2SO_4$ and 1N HCl in the presence and absence of the inhibitor compounds has been investigated using EIS at room temperature. Nyquist plots of mild steel in uninhibited and inhibited acid solution containing various concentrations of F3MPO, F3IPPO, F3DMPO and FDMPO are given in Figures 4, 5, 6,7 and 8. As all the inhibitors gave similar spectra only representative plots are given. A single capacitative loop is observed at all concentrations from 0.1 mM to 5 mM and all the impedance spectra have been measured at the respective corrosion potential and analysed in terms of an Randles equivalent circuit with the help of Ivium software. These circuits fall into the classical parallel resistor capacitor combination, the series resistor being that of the solution. In the circuit, $R_s$ represents the solution resistance and $R_{ct}$ the polarization resistance and Q a constant phase element (CPE) whose admittantance is defined as $Q = Y_o (j2\pi f)^n$

The inhibition efficiencies were calculated from the $R_{ct}$ data using the formula given below and are shown in Tables 7 and 8.

$$IE(\%) = \left( \frac{R_{ct(inh)} - R_{ct\ (Blank)}}{R_{ct(inh)}} \right) \times 100 \quad (2)$$

Where $R_{ct(inh)}$ is the charge transfer resistance for inhibited solution and $R_{ct\ (Blank)}$ is the charge transfer resistance for uninhibited solution.

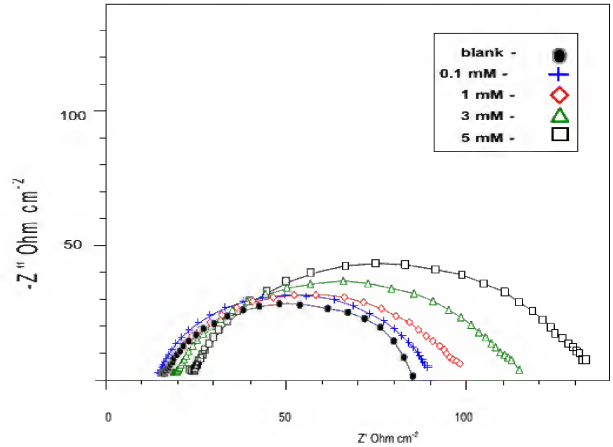


**Figure 4: The Nyquist Plots for MS in 1N $H_2SO_4$ in the Presence and in the Absence of F3MPO**

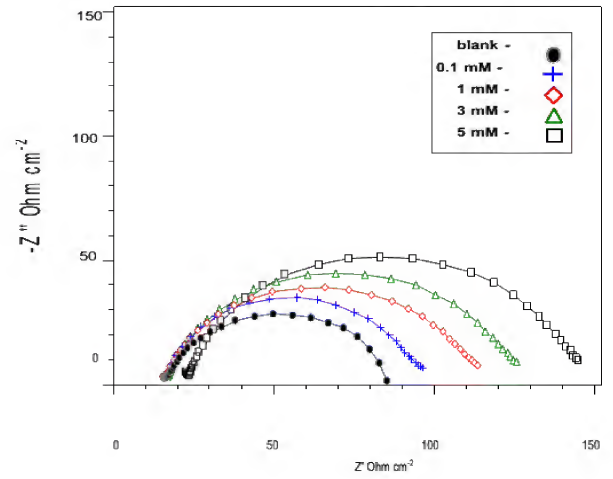


**Figure 5: The Nyquist Plots for MS in 1N $H_2SO_4$ in the Presence and in the Absence of FDMPO**

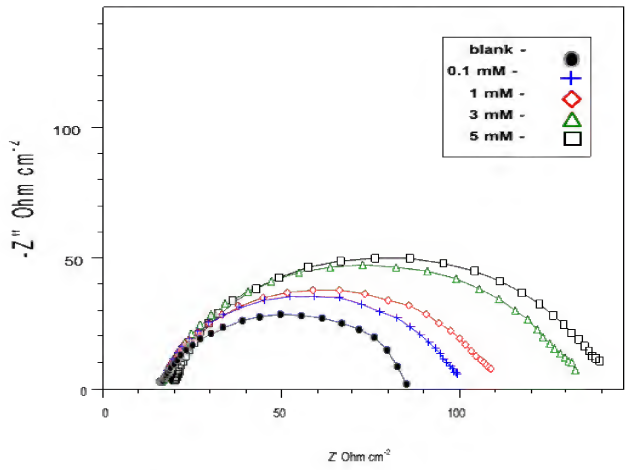


**Figure 6: The Nyquist Plots for MS in 1N $H_2SO_4$ in the Presence and in the Absence of F3DMPO**

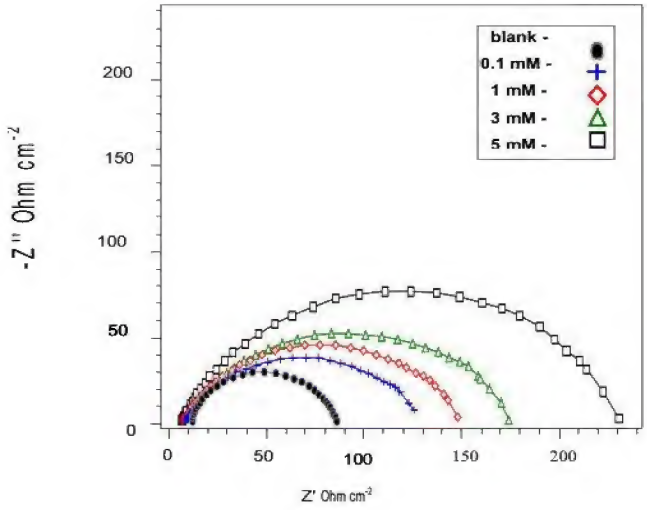


**Figure 7: The Nyquist Plots for MS in 1N HCl in the Presence and in the Absence of F3DMPO**

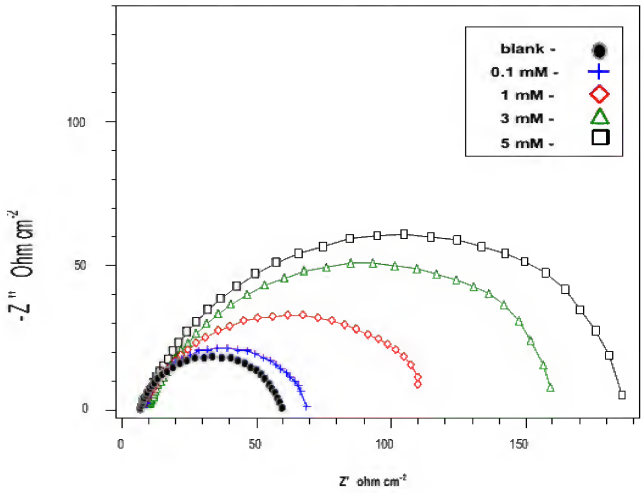


**Figure 8: The Nyquist Plots for MS in 1N HCl in the Presence and in the Absence of F3IPPO**

The increase in $R_{ct}$ values with an increase in inhibitor concentration is the result of an increase in the surface coverage by the inhibitor molecule which led to increase in inhibitor efficiency. The decrease in the $C_{dl}$ values with the increase in inhibitor concentration is due to the adsorption of the inhibitor molecule replacing water molecule at the metal-solution interface that led to the decrease in local dielectric constant and /or an increase in thickness of the electrical double layer[18]. Hence the change in $C_{dl}$ values which is caused by the gradual displacement of water molecule by the adsorption of the inhibitor at the metal-solution interface decreases the extent of the corrosion[19]. The efficiency of all inhibitors increases with the increase in concentration and shows the same trend as in gravimetric measurements F3IPPO>F3MPO>F3DMPO>FDMPO in both the media.

**Potentiostatic Polarization Study**

Figures 9, 10,11,12 and 13 show polarization curves of mild steel in 1N $H_2SO_4$ and 1N HCl in the presence and absence of various concentration of F3MPO, F3IPPO, F3DMPO and FDMPO. It is obvious that the addition of inhibitors hindered the acid attack on the mild steel electrode and increasing the concentration of the inhibitor gave rise to a consistent decrease in anodic and cathodic current densities indicating that F3MPO, F3IPPO, F3DMPO and FDMPO act as a mixed type inhibitors[20].

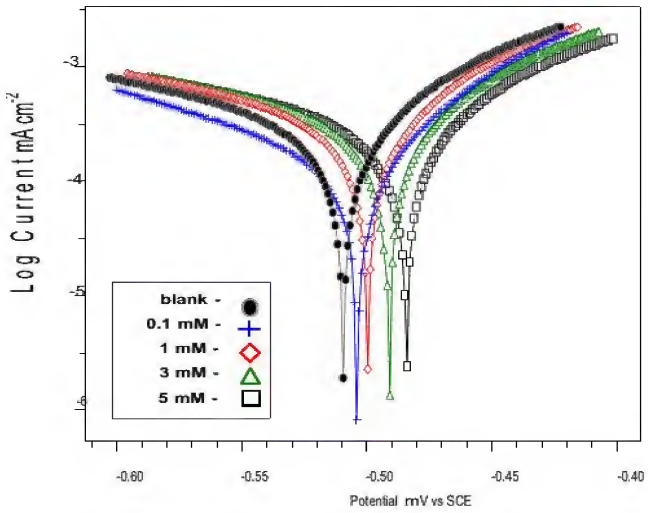


**Figure 9: The Tafel Plots for MS in 1N $H_2SO_4$ in the Presence and in the Absence of F3MPO**

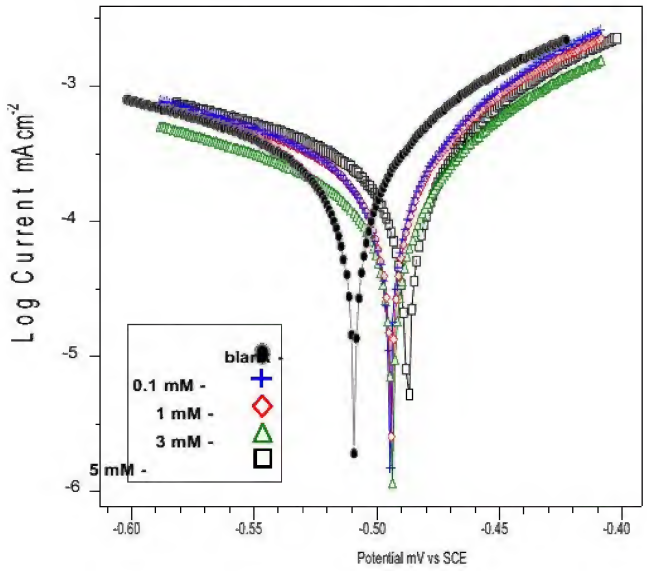


**Figure 10: The Tafel Plots for MS in 1N $H_2SO_4$ in the Presence and in the Absence of FDMPO**

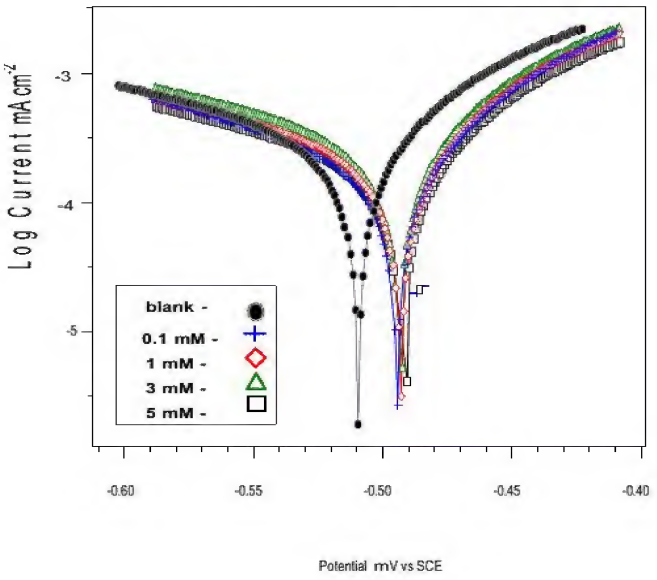


**Figure 11: The Tafel Plots for MS in 1N $H_2SO_4$ in the Presence and in the Absence of F3DMPO**

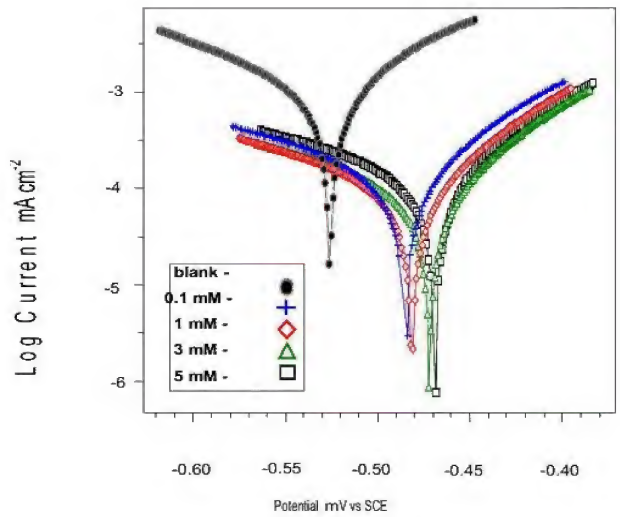


**Figure 12: The Tafel Plots for MS in 1N HCl in the Presence and in the Absence of F3DMPO**

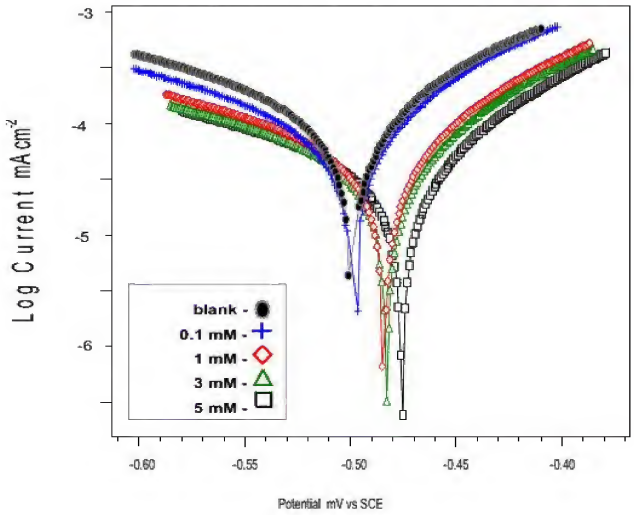


**Figure 13: The Tafel Plots for MS in 1N HCl in the Presence and in the Absence of F3IPPO**

The corrosion potential ($E_{cor}$), corrosion current density ($I_{cor}$), Tafel slope $\beta_a$ , $\beta_c$ which are obtained by extrapolation of the Tafel lines are listed in Tables 7 and 8. The calculated percentage inhibition efficiency (IE%) are also given in Tables 7 and 8. Analysis of these data shows that $I_{corr}$ decreased with the addition of inhibitors in 1N $H_2SO_4$ and 1N HCl due to the increase in the blocked fraction of the electrode surface by adsorption. The $E_{corr}$ value is also shifted towards the more noble side with an increase in the inhibitor concentration.

**Adsorption Isotherm**

In order to understand the mechanism and nature of adsorption attempts were made to fit surface coverage values θ to various isotherms including Frumkin, Langmuir and Temkin. The best fit was obtained with both the Langmuir and Tempkin Isotherms (Figures 14,15,16 and 17). According to Langmuir isotherm, θ is related to concentration of the inhibitor $C_{inh}$ *via*

$$\frac{\theta}{1-\theta} = kC_{inh} \exp\left(\frac{-\Delta G^{\circ}_{ads}}{RT}\right) \quad (3)$$

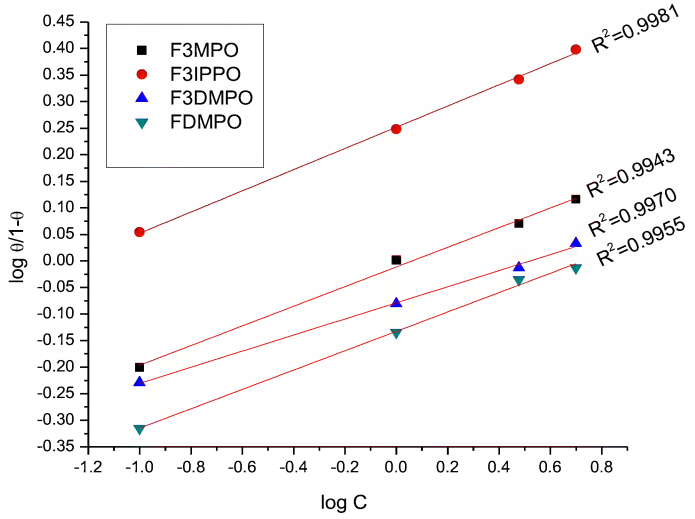


**Figure 14: The Langmuir Isotherms for the Adsorption of Inhibitors in 1N $H_2SO_4$ Solution**

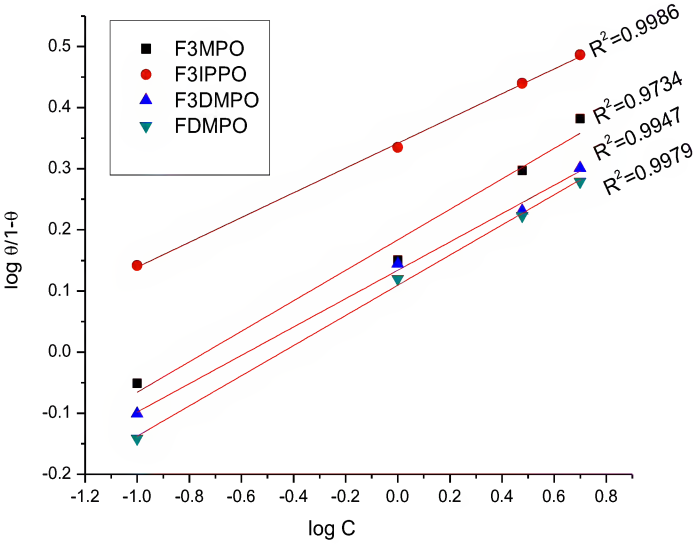


**Figure 15: The Langmuir Isotherms for the Adsorption of Inhibitors in 1N HCl Solution**

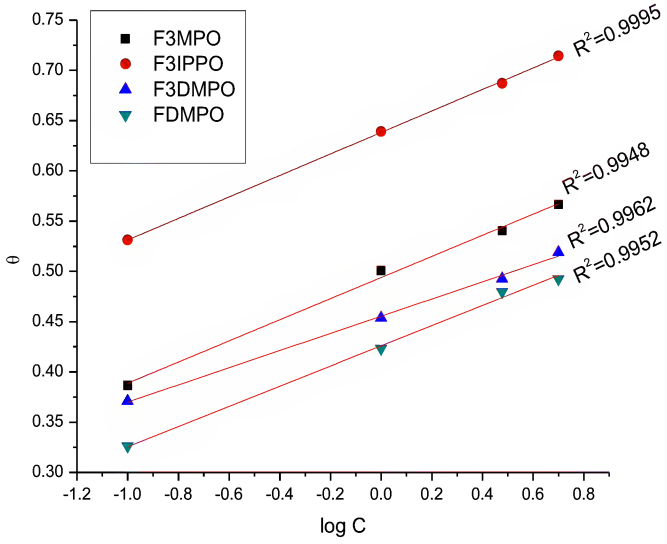


**Figure 16: The Tempkin Isotherms for the Adsorption of Inhibitors in 1N $H_2SO_4$ Solution**

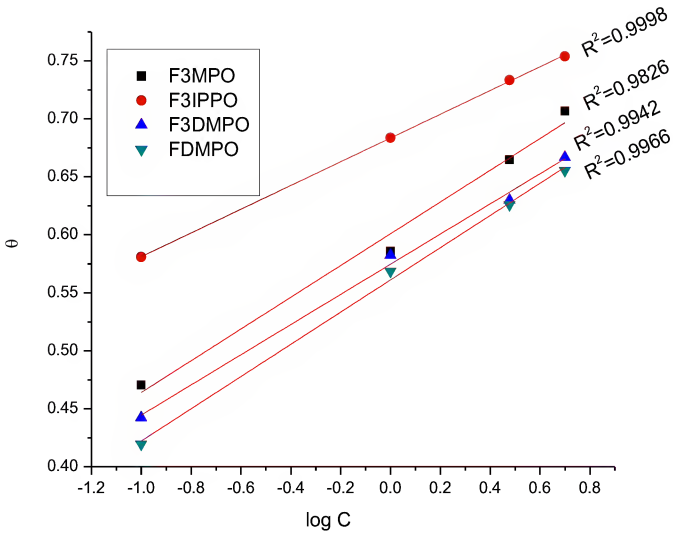


**Figure 17: The Tempkin Isotherms for the Adsorption of Inhibitors in 1N HCl Solution**

This equation predicts a linear plot between the values of log (θ/1-θ) and log $C_{inh}$, $\Delta G^{\circ}_{ads}$ is the free energy of adsorption and K is the constant[21]. The strong correlation ($r^2$ = 0.9911) in 1N HCl and ($r^2$ = 0.9962) in 1N $H_2SO_4$ for the Langmuir adsorption isotherm for the inhibitors confirms the validity of this approach. Like many organic inhibitors *N*-formyl piperidin-4-ones also follows Tempkin's Isotherm with a high correlation ($r^2$ = 0.9933) in 1N HCl and ($r^2$ = 0.9964) in 1N $H_2SO_4$.

## DISCUSSIONS

As far as the inhibition process is concerned it is generally assumed that adsorption of the inhibitor at the metal-solution interface is the first step in the mechanism of inhibitors in aggressive media. Four types of adsorption may take place involving organic molecules at the metal-solution interface: (1) electrostatic attraction between charged molecules and the charged metal, (2) the interaction of unshared electron pairs in the molecule with the metal, (3) interaction of π electrons with the metal and (4) a combination of the above[22].

Chemisorption involves charge sharing or charge transfer from the inhibitor molecule to the mild steel surface to form a coordinate covalent type bond. The electron transfer is reckoned for transition metals having vacant, low-energy electron orbital. Inhibition efficiency depends on several factors such as the number of adsorption sites and their charge density, molecular size of the inhibitor molecule, mode of interaction with the metal surface and formation of metallic complexes [23].

The *N*-formyl inhibitor interferes in the dissolution reaction by adsorption on metal surface in two different ways. First, the inhibitor competes with $Cl^-$ or $SO_4^{2-}$ ions for anodic sites which are originally water covered. In the process of adsorption, the protonated inhibitor loses its associated proton(s) in entering the double layer and chemisorbs by donating electrons to the metal. In addition, the protonated inhibitor electrostatically adsorbs on to the anion covered surface through its cationic form. *N*-formyl inhibitor thus plays a predominant role by participating in a number of adsorption – desorption steps, rather than by a mere blockage of sites [16, 24, 25].

The binding character of inhibitor on the mild steel surface can be interpreted by means of coordination bonds using electron pairs of oxygen atom and π electrons of the benzene ring. Better corrosion inhibition can be obtained

through the formation of true chemical bonds between organic molecule and metal surface. Hence it can be concluded that inhibition of corrosion of mild steel by *N*-formyl piperidin-4-ones in aggressive medium is due to the adsorption of $Fe^{+2}$ – inhibitor complex, coordinated with electron pairs of oxygen atoms of both the carbonyl groups.

As chloride ions are more strongly adsorbed on the iron surface than sulphate ions, the cationic form of the formyl inhibitor molecule can adsorb on the metal surface with relative ease in HCl compared with $H_2SO_4$ [18, 20] thus accounting the high inhibitor efficiency in HCl medium than in $H_2SO_4$.

As the process of inhibition occurs through the phenomenon of adsorption, it is necessary to develop suitable mechanism for the adsorption of *N*-formyl piperidin-4-ones on the carbon steel surface. Damaskin *et al.*[26] suggested that the adsorption of organic molecule on different type of metallic surfaces occurs through competitive adsorption between organic compound and water molecules. The higher free energy of adsorption for organic compounds than for water molecule facilitates such adsorption. Sankarapapavinasam *et al.*[12] have analysed the adsorption of piperidine and few piperidones *viz.* 2,6-diphenylpiperidin-4-one, 3-methyl-2,6-diphenylpiperidin-4-one, 2,2-dimethyl-2,6-diphenylpiperidin-4-one on the corrosion of copper and sulphuric acid. They have proposed that the interaction of piperidone with the metal surface could occur through >C=O or –NH group. The lower electronegativity of the nitrogen atom favours NH as an anchoring site with chair conformation, but involvement of both groups was ruled out by them as it would need the piperidones to be in strained boat conformation. Muralidharan et al.[20] and Mallika et al.[27] have also concluded that piperidones adsorb through nitrogen lone pair in chair conformation.

However, Ravichandran *et al.*[28] have proposed that the piperidin-4-ones adsorbed through both - NH and >C=O groups at positions 1 and 4, respectively, with strained boat conformation using IR spectral studies. The carbonyl adsorption peak around 1700 $cm^{-1}$ has disappeared completely when N-H stretching band around 3000-3500 $cm^{-1}$ and C-N stretching around 1000-1350 $cm^{-1}$ have been altered. A new O-H stretching band at 3000-3500 $cm^{-1}$ has appeared. They also proposed that after adsorption on mild steel surface, the carbonyl group is reduced catalytically to C-OH group to axial alcohol to facilitate the continued adsorption in the boat form.

Jeyaraman *et al.* [3] have shown that the preferred conformation of *N*-formyl-*cis*-2,6-diaryl piperidin-4-ones in solution were found to be flattened boat with the aryl groups in quasi-axial position which is shown in Figure 18. The severe $A^{1,3}$ strain due the interaction between –N-C=O group (coplanar to C2-N1-C6 plane) and the adjacent phenyl groups forces the *N*-formyl-*cis*-2,6-diarylpiperidin-4-ones to prefer flattened boat conformation. They also averred that a hydrogen bond type of attraction between the electron rich oxygen atom of –N-C=O group and the electron deficient hydrogen at α-position stabilises the flattened boat conformation

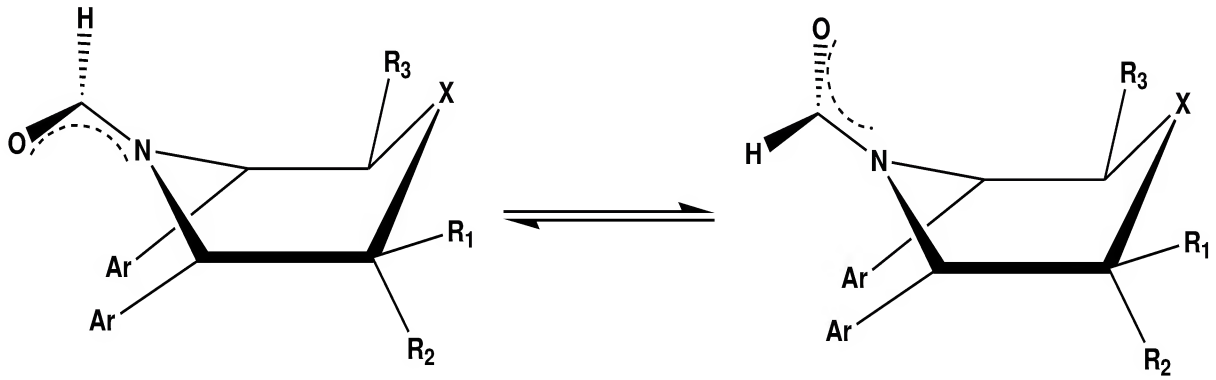

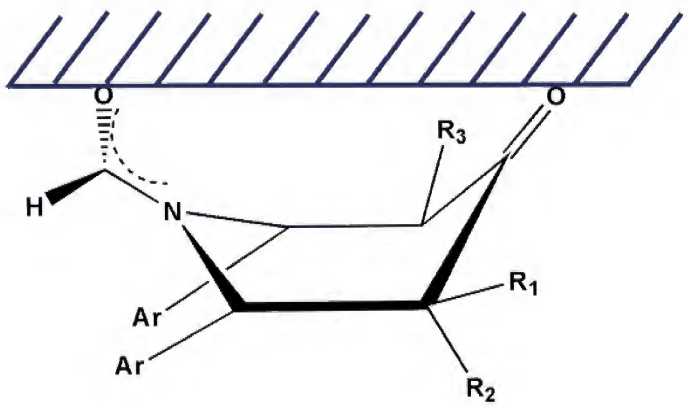


**Figure 18: Mode of Adsorption of *N*-Formylpiperidin-4-Ones in the Flattened Boat Conformation**

The FT-IR spectra of F3MPO, F3IPPO, F3DMPO and FDMPO are recorded using Perkin-Elmer 1600 FT-IR spectrometer and are shown in Figures 19 (a) to 22 (a), respectively. FT-IR spectra of the adsorbed material scratched from the metal surface is shown in Figures 19 (b) to 22 (b). On careful observation of FT-IR spectra it is evident that the carbonyl frequency of the amide group appeared around 1660 $cm^{-1}$ and the carbonyl frequency of the ring group appeared at 1710 $cm^{-1}$ were absent and shifted down to 1503 $cm^{-1}$ - 1530 $cm^{-1}$. These shifts in >C=O stretching can be attributed to the shift of electron density of the >C=O towards $Fe^{+2}$ resulting in the formation of $Fe^{+2}$ – inhibitor complex thus controlling the corrosion. Moreover the carbonyl group gets reduced to alcohol and continues to be adsorbed on the MS surface whose stretching frequency shifted higher to 3500 $cm^{-1}$ - 3700 $cm^{-1}$ in the product molecule. The mechanism of inhibition is portrayed in Figure 18.

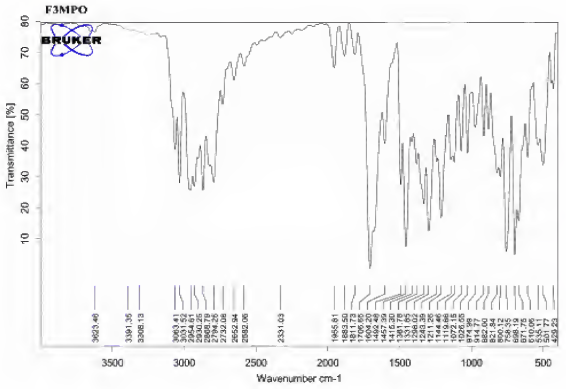


**Figure 19: (a) F3MPO**

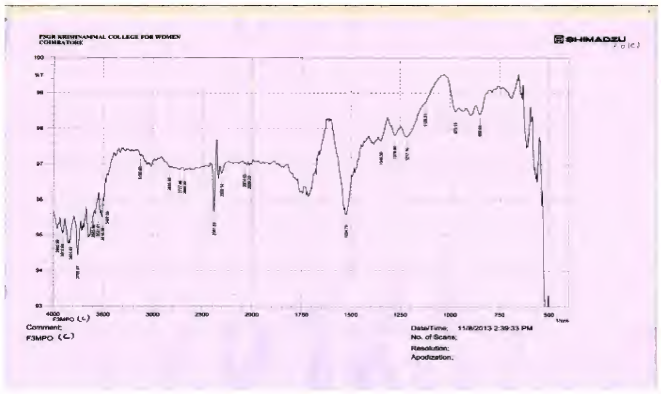

**Figure 19: (b) F3MPO (Compound)**

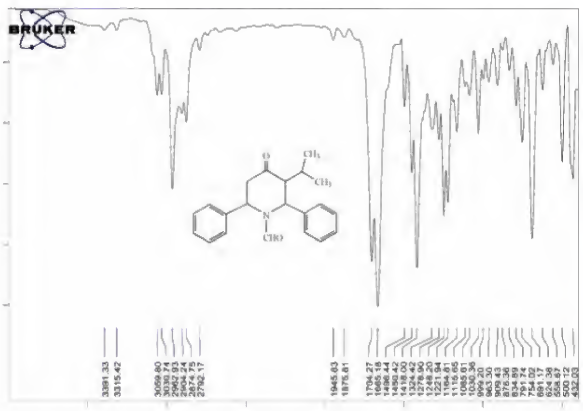


**Figure 20: (a) F3IPPO**

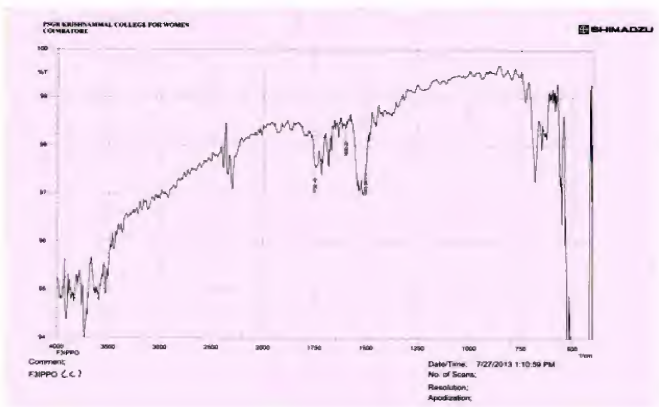

**Figure 20: (b) F3IPPO (Compound)**

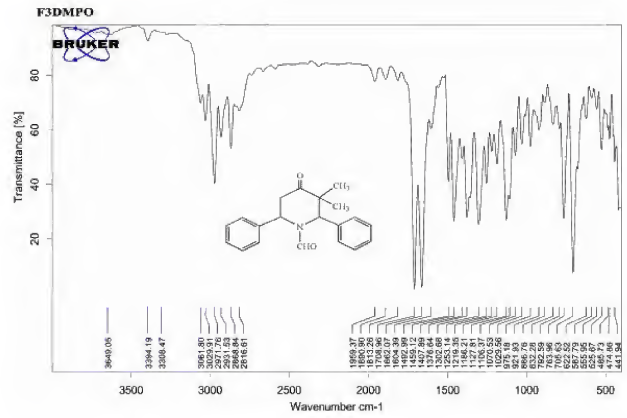


**Figure 21: (a) F3DMPO**

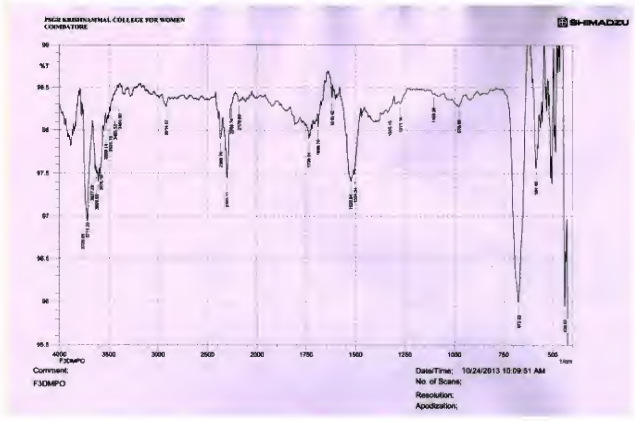


**Figure 21: (b) F3DMPO (Compound)**

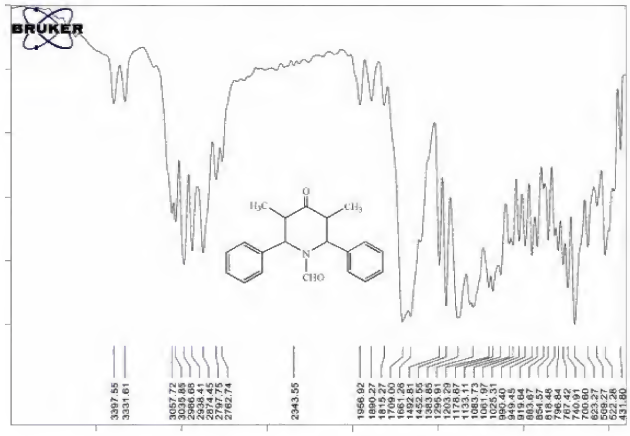


**Figure 22: (a) FDMPO**

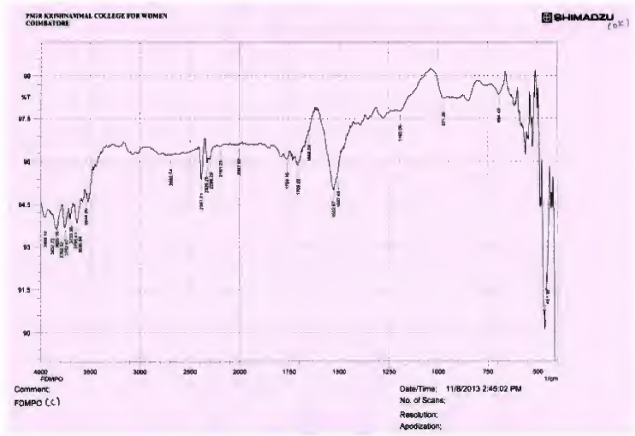


**Figure 22: (b) FDMPO (Compound)**

**Surface Analysis**

The surface morphology was studied by SEM and EDS and given in Figures 23(a), 23(b), 23(c), and 23(d). The uninhibited SEM picture [23(a)] shows the distribution of corrosion products on the surface and the inhibited SEM picture [23(b)] vividly shows the presence of adsorbed inhibitor molecule on the surface thus preventing corrosion.

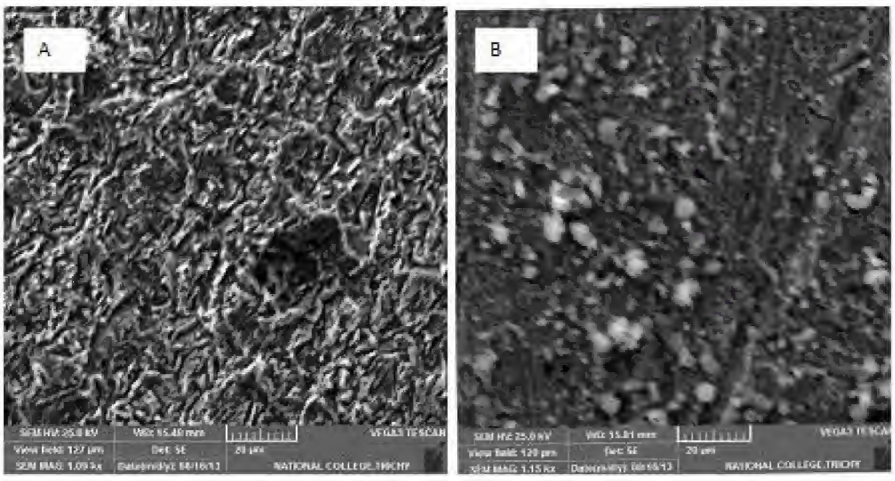


**Figures 23: Show the SEM Image of Uninhibited MS Surface (A) MS Surface Inhibited by FDMPO (B)**

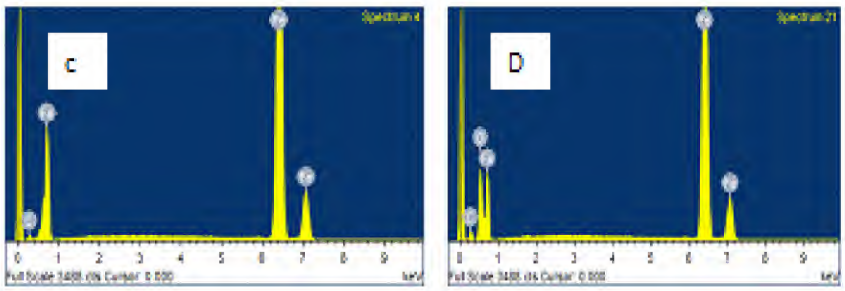


**Figure 24**

| Element | Weight % | Atomic% |
|---|---|---|
| C | 9.32 | 23.49 |
| O | 20.24 | 38.31 |
| Fe | 70.45 | 38.20 |
| Total | 100 | |

| Element | Weight % | Atomic% |
|---|---|---|
| C | 6.51 | 24.46 |
| Fe | 93.49 | 75.54 |
| Total | 100 | |

## CONCLUSIONS

All the *N*-formyl derivatives of piperidine-4-ones show good inhibition efficiency in both 1N $H_2SO_4$ and 1N HCl medium. The inhibition efficiency of the *N*-formyl piperidin-4-ones follows the order: F3IPPO > F3MPO > F3DMPO > FDMPO. The protection efficiency increases with the increase in concentration and reaches a maximum of 5 mM concentration. The polarization studies show that the inhibitors suppress both anodic and cathodic corrosion and thus act as mixed inhibitors. The single loop in the electrochemical impedance spectroscopy shows that the inhibition is by adsorption of the inhibitor on the mild steel surface and blocking the active sites. FT-IR spectra show that the adsorbed material consists of $Fe^{+2}$ – inhibitor complex. The adsorption of inhibitor correlates well with both Langmuir and Tempkin adsorption Isotherms. The inhibition efficiency increases with the increase in temperature up to 323K and immersion time 12 h.

## REFERENCES

1. G. Trabanelli, *Corrosion* **47** (1991) 410.
2. T. Ravindran, R. Jeyaraman, R. W. Murray and M. Singh, M. *J. Org. Chem.* **56** (1991) 4833.
3. R. Jeyaraman, J. C. Thenmozhiyal, R. Murugadoss and M. Venkatraj,. *Indian J. Chem.* **38B** (1999) 325.
4. P. Sakthivel, Ph.D. Thesis, Bharathiar University, India (2014).
5. C. R. Noller and V. Baliah, V. *J. Am. Chem. Soc.,* 70 (1948) 3853.
6. S. Ponnuswamy, R. Murugadoss, R. Jeyaraman, A. Thiruvalluvar and V. parthasarathy *Indian J. Chem.* **45B** (2006) 2059.
7. K. Ravichandran, P. Sakthivel, P. Ramesh, S. Ponnuswamy and M. N. Ponnuswamy *Acta Cryst.* **E68** (2012) 0870.

8. K. Ravichandran, P. Ramesh, P. Sakthivel, S. Ponnuswamy and M. N. Ponnuswamy *Acta Cryst.* **E66** (2010) 1505.
9. T. kavitha, P. Sakthivel, S. Ponnuswamy, S. S. Ilango and M. N. Ponnuswamy *Acta Cryst.* **E65** (2009) 2818.
10. S. Ponnuswamy, M. Venkatraj, R. Jeyaraman, M. Sureshkumar, D. Kumaran, D and M. N. Ponnuswamy *Indian J. Chem.* **41B** (2002) 614.
11. F. Bentiss, M.Traisnel, M.Lagrenee, *Corros. Sci.* **42** (2009) 127.
12. Sankarapapavinasam, F. Pushpanathan and M. F. Ahmed, *Corros. Sci..,* **32** (1989) 193.
13. R.S. Chaudhary, S. Ind. Sharma, *J.Chem. Technol.* **6** (1999) 202.
14. S.A. Umoren, I.B. Obot, E.E. Ebenso and N.O. obi-Egbedi, *Desalination*. **250** (2009) 225
15. N. Hackermann, E.S. Snavel and J.S. Payne, *J. Electrochem. Soc.,* **113** (1966) 677.
16. N. Hackermann and E. McCafferty, *Proceedings of the 5th international Congress on "Metalic Corrosion"* (Tokyo, 1972), p. 542
17. H. B. Rudresh and S.M. Mayanna, *J. Electrochem. Soc. India,* **31** (1982) 109.
18. M. Behpour, S.M. Ghoreshi, A. Gandomi-Niasar, N. Soltani and M. Salavati-Niasari, *J. Mater. Sci.* **44** (2009) 2444.
19. M. Benabdellah, R. Touzani, A. Aouniti. A. Dafali, S. El Kadiri, B. Hammoutia and M. Benkadddour, *Mater. Chem. Phys.* **105** (2007) 373.
20. S. Muralidharan, K.L.N. Phani, S. Pitchumani, S. Ravichhandran and S.V.K. Iyer, *J. Electrochem. Soc.* **142** (1995) 1478.
21. S. Kertit and B. Hammouti, *Appl. Surf. Sci.* **93** (1996) 59.
22. F. Bentiss, M. Traisnel, M. Lagrenee, *J. Applied Electrochem.* **31** (2001) 41.
23. A. Fouda, M. Moussa, F. Taha and El Neanaa, *Corros. Sci.* **26** (1986) 719.
24. N. Hackermann, E.S. Snavel, Jr and J.S. Payne, Jr, *J. Electrochem. Soc.* **113** (1966) 677.
25. T. Murakawa and N. Hackermann, *Corros. Sci.* **4** (1964) 387.
26. Boris B. Damaskin, Oleg A. Petrii and Valerii. V. Batrakov, "*Adsorption of Organic Compounds on Electrodes*", Plenum Press, New York, London, (1971) 262 – 266.
27. J. Mallika, Ph.D. Thesis, Bharathiyar University, India (2002).
28. J. Ravichandran, Ph.D. Thesis, Bharathiyar University, India (2006).

## APPENDICES

**Table 1: Inhibiting Efficiency from Weight Loss Measurements**

| Inhibitor+40 ml Ethyl Alcohol. | Concentration (mM) | $H_2SO_4$ | | | HCl | | |
|---|---|---|---|---|---|---|---|
| | | Weight Loss (mg) | Corrosion Rate (mm /y) | IE% | Weight Loss (mg) | Corrosion Rate (mm /y) | IE% |
| F3MPO | Blank: + 40 ml ethyl alcohol | 7.715 | 11.436 | | 10.95 | 16.232 | |
| | 0.1 | 4.733 | 7.0162 | 38.65 | 5.791 | 8.5846 | 47.05 |
| | 1.0 | 3.852 | 5.7102 | 50.07 | 4.535 | 6.7227 | 58.58 |
| | 3.0 | 3.546 | 5.2566 | 54.04 | 3.671 | 5.4419 | 66.48 |
| | 5.0 | 3.343 | 4.9557 | 56.66 | 3.211 | 4.7600 | 70.68 |
| F3IPPO | 0.1 | 3.617 | 5.3618 | 53.12 | 4.589 | 6.8027 | 58.09 |
| | 1.0 | 2.784 | 4.1270 | 63.91 | 3.463 | 5.1336 | 68.37 |
| | 3.0 | 2.413 | 3.5770 | 68.72 | 2.918 | 4.3256 | 73.35 |
| | 5.0 | 2.204 | 3.2672 | 71.43 | 2.694 | 3.9936 | 75.4 |
| F3DMPO | 0.1 | 4.852 | 7.1926 | 37.11 | 6.107 | 9.0530 | 44.23 |
| | 1.0 | 4.213 | 6.2454 | 45.39 | 4.473 | 6.6308 | 58.24 |
| | 3.0 | 3.914 | 5.8021 | 49.27 | 4.051 | 6.0052 | 63 |
| | 5.0 | 3.712 | 5.5027 | 51.91 | 3.647 | 5.4063 | 66.69 |
| FDMPO | 0.1 | 5.200 | 7.7085 | 32.6 | 6.358 | 9.4251 | 41.94 |
| | 1.0 | 4.453 | 6.6011 | 42.32 | 4.724 | 7.0029 | 56.86 |
| | 3.0 | 4.014 | 5.9504 | 47.97 | 4.098 | 6.0749 | 62.58 |
| | 5.0 | 3.915 | 5.8036 | 49.25 | 3.774 | 5.5946 | 65.53 |

**Table 2: Effect of Immersion Period on the 1mM Inhibitors of the Corrosion of MS in $H_2SO_4$ Media**

| Immersion Period in h | Blank CR (mm/y) | F3MPO | | F3IPPO | | F3DMPO | | FDMPO | |
|---|---|---|---|---|---|---|---|---|---|
| | | CR (mm/y) | IE(%) | CR (mm/y) | IE(%) | CR (mm/y) | IE(%) | CR (mm/y) | IE(%) |
| 1 | 9.051 | 6.419 | 29.080 | 5.606 | 38.062 | 7.770 | 14.153 | 7.924 | 12.452 |
| 3 | 17.184 | 10.102 | 41.213 | 8.991 | 47.678 | 11.516 | 32.984 | 11.977 | 30.301 |
| 6 | 32.38 | 15.626 | 51.742 | 14.070 | 56.547 | 17.137 | 47.075 | 18.058 | 44.231 |
| 9 | 47.582 | 21.150 | 55.550 | 19.148 | 59.758 | 22.757 | 52.173 | 24.139 | 49.269 |
| 12 | 62.782 | 26.674 | 57.513 | 24.226 | 61.413 | 28.377 | 54.801 | 30.220 | 51.865 |
| 24 | 123.579 | 50.769 | 58.918 | 46.538 | 62.341 | 54.859 | 55.608 | 58.543 | 52.627 |

**Table 3: Effect of Addition of 1mM Anions on the Corrosion Inhibition of MS in 1N $H_2SO_4$**

| System | (1mMF3MPO) | | | (1mM F3IPPO) | | | (1mM F3DMPO) | | | (1mM FDMPO) | | |
|---|---|---|---|---|---|---|---|---|---|---|---|---|
| | Weight Loss (mg) | Corrosion Rate (mm/y) | IE (%) | Weight Loss (mg) | Corrosion Rate (mm/y) | IE (%) | Weight Loss (mg) | Corrosion Rate (mm/y) | IE (%) | Weight Loss (mg) | Corrosion Rate (mm/y) | IE (%) |
| Blank | 4.833 | 7.164 | | 4.492 | 6.658 | | 5.33 | 7.9 | | 5.66 | 8.39 | |
| $KNO_3$ | 4.166 | 6.176 | 13.80 | 4.147 | 6.148 | 7.68 | 4.29 | 6.359 | 11.51 | 5.00 | 7.412 | 11.65 |
| KCNS | 4.00 | 5.92 | 17.23 | 3.942 | 5.844 | 12.24 | 4.46 | 6.612 | 16.32 | 4.92 | 7.293 | 13.18 |
| KCl | 3.66 | 5.434 | 24.14 | 3.82 | 5.663 | 14.96 | 4.38 | 6.49 | 17.82 | 4.66 | 6.908 | 17.668 |
| $KBrO_3$ | 3.166 | 4.694 | 34.47 | 3.41 | 5.055 | 24.08 | 3.56 | 5.277 | 33.21 | 3.9 | 5.781 | 31.09 |
| KBr | 2.833 | 4.199 | 41.37 | 3.00 | 4.447 | 33.21 | 2.89 | 4.284 | 45.78 | 3.83 | 5.677 | 32.33 |
| KI | 1.833 | 2.717 | 62.07 | 1.923 | 2.853 | 57.19 | 2.39 | 3.543 | 55.16 | 3.00 | 4.447 | 46.998 |

**Table 4: Effect of the Temperature and Corrosion Inhibition of MS in $H_2SO_4$ Medium**

| System | 303K | | 308K | | 313K | | 318K | | 323K | |
|---|---|---|---|---|---|---|---|---|---|---|
| | CR (mm/y) | IE (%) | CR (mm/y) | IE (%) | CR (mm/y) | IE (%) | CR (mm/y) | IE (%) | CR (mm/y) | IE (%) |
| Blank | 13.319 | - | 23.00 | - | 32.367 | - | 41.423 | - | 50.245 | - |
| F3MPO | 8.993 | 32.48 | 12.904 | 43.90 | 16.694 | 48.42 | 20.362 | 50.84 | 23.919 | 52.40 |
| F3IPPO | 8.455 | 36.59 | 12.048 | 47.62 | 15.639 | 51.68 | 18.927 | 54.307 | 22.241 | 55.73 |
| F3DMPO | 9.455 | 29.02 | 13.728 | 40.31 | 17.875 | 44.78 | 21.869 | 47.205 | 25.754 | 48.74 |
| FDMPO | 10.149 | 23.80 | 14.697 | 36.10 | 19.121 | 40.92 | 23.367 | 43.589 | 27.502 | 45.26 |

**Table 5: Thermodynamic Parameter**

| Inhibitor | $E_a$ (KJmol$^{-1}$) | $\Delta H^{\#}$(KJmol$^{-1}$) | $\Delta S^{\#}$(JK$^{-1}$mol$^{-1}$) |
|---|---|---|---|
| BLANK | 52.995 | 50.394 | -56.251 |
| F3MPO | 39.379 | 36.778 | -104.91 |
| F3IPPO | 38.948 | 36.347 | -106.851 |
| F3DMPO | 40.318 | 37.717 | -101.361 |
| FDMPO | 40.115 | 37.515 | -101.446 |

**Table 6: $\Delta G^{O}$ (KJmol$^{-1}$)**

| Inhibitor | 303K | 308K | 313K | 318K | 323K |
|---|---|---|---|---|---|
| F3MPO | -8.276 | -9.658 | -10.289 | -10.709 | -11.045 |
| F3IPPO | -8.734 | -9.880 | -10.629 | -11.078 | -11.406 |
| F3DMPO | -7.866 | -9.130 | -9.908 | -10.325 | -10.652 |
| FDMPO | -7.188 | -8.681 | -9.498 | -9.939 | -10.277 |

**Table 7: Electrochemical Parameters for MS Corrosion in 1 N $H_2SO_4$ + 40 ml Ethyl Alcohol with Different Concentrations of the Inhibitor**

| | Conc. of Inhibitor (mM) | $R_{ct}$ Ohm cm$^2$ | $C_{dl}$ (F) *10$^{-5}$ | IE (%) | $\beta_a$ (mV) | $\beta_c$ (mV) | $I_{corr}$ (µA/CM$^2$) | -$E_{corr}$ (mV) | Corrosion Rate (mm/y) | $R_p$ Ohm | IE (%) |
|---|---|---|---|---|---|---|---|---|---|---|---|
| | BLANK | 29.39 | 3.09 | | 78 | 145 | 373.8 | 511.1 | 5.596 | 102.3 | |
| F3MPO | 0.1 | 60.0 | 3.37 | 51.02 | 80 | 163 | 241.8 | 504.1 | 6.1 | 94.39 | 35.31 |
| | 1 | 66.6 | 3.31 | 55.87 | 79 | 153 | 203.2 | 499.9 | 5.995 | 99.29 | 45.63 |
| | 3 | 87.3 | 3.09 | 66.36 | 76 | 156 | 168.0 | 491.5 | 5.64 | 107.9 | 55.06 |
| | 5 | 94.0 | 2.66 | 68.73 | 62 | 126 | 151.7 | 484.0 | 4.1 | 152 | 59.42 |
| F3IPPO | 0.1 | 64.2 | 3.51 | 54.22 | 78 | 156 | 232.6 | 507.6 | 5.56 | 104.2 | 37.77 |
| | 1 | 73.4 | 3.42 | 59.96 | 74 | 152 | 201.3 | 498.6 | 4.72 | 121.6 | 46.15 |
| | 3 | 91.6 | 3.02 | 67.91 | 73 | 140 | 162.1 | 494.3 | 3.89 | 143.2 | 56.63 |
| | 5 | 104.6 | 2.56 | 71.90 | 63 | 133 | 120.2 | 490.2 | 3.72 | 162.3 | 67.84 |
| F3DMPO | 0.1 | 56.8 | 2.75 | 48.25 | 76 | 154 | 253.6 | 503.2 | 5.58 | 106.2 | 32.16 |
| | 1 | 68.6 | 2.91 | 57.15 | 73 | 153 | 205.6 | 498.1 | 4.61 | 129.2 | 44.50 |
| | 3 | 80.3 | 2.69 | 63.40 | 72 | 152 | 173.2 | 493.2 | 3.989 | 152.6 | 53.67 |
| | 5 | 90.2 | 2.64 | 67.41 | 67 | 130 | 165.2 | 490.4 | 3.85 | 161.4 | 55.81 |
| FDMPO | 0.1 | 54.8 | 3.89 | 46.37 | 76 | 154 | 273.3 | 495.8 | 3.85 | 102.8 | 26.89 |
| | 1 | 66.6 | 2.98 | 55.87 | 72 | 153 | 225.6 | 495.1 | 3.989 | 120.8 | 39.65 |
| | 3 | 81.4 | 2.89 | 63.89 | 67 | 153 | 195.2 | 494.1 | 4.61 | 133.0 | 47.78 |
| | 5 | 87.8 | 2.50 | 66.53 | 73 | 130 | 188.4 | 494.6 | 5.586 | 141.1 | 49.59 |

**Table 8: Electrochemical Parameters for MS Corrosion in 1N HCl + 40 ml Ethyl Alcohol with Different Concentrations of the Inhibitor**

| | Conc. of Inhibitor (mM) | $R_{ct}$ Ohm cm$^2$ | $C_{dl}$ (F) *10$^{-5}$ | IE (%) | $\beta_a$ (mV) | $\beta_c$ (mV) | $I_{corr}$ (µA/CM$^2$) | -$E_{corr}$ (mV) | Corrosion Rate (mm/y) | $R_p$ Ohm | IE (%) |
|---|---|---|---|---|---|---|---|---|---|---|---|
| | BLANK | 34.3 | 7.34 | | 81 | 133 | 313.7 | 496.8 | 1.026 | 89.43 | |
| F3MPO | 0.1 | 60.1 | 7.78 | 42.93 | 81 | 140 | 200.6 | 496.6 | 0.7992 | 114.9 | 36.05 |
| | 1 | 87.2 | 5.37 | 60.67 | 78 | 139 | 144.0 | 484.3 | 0.504 | 180.6 | 45.41 |
| | 3 | 108.3 | 4.38 | 68.33 | 75 | 137 | 122.6 | 482.7 | 0.4154 | 213.4 | 60.92 |
| | 5 | 133.5 | 4.09 | 74.31 | 74 | 136 | 107.6 | 475.9 | 0.3522 | 248.4 | 65.70 |
| F3IPPO | 0.1 | 82.6 | 5.73 | 58.47 | 69 | 142 | 124.6 | 482.8 | 1.894 | 203.2 | 60.28 |
| | 1 | 100.8 | 5.24 | 65.97 | 66 | 133 | 101.8 | 479.3 | 1.851 | 211.4 | 67.55 |
| | 3 | 117.8 | 5.43 | 70.88 | 65 | 135 | 90.5 | 470.0 | 1.375 | 269.7 | 71.15 |
| | 5 | 172.1 | 4.51 | 80.07 | 69 | 135 | 83.8 | 467.2 | 1.274 | 289.6 | 73.29 |
| F3DMPO | 0.1 | 62.4 | 5.73 | 45.03 | 78 | 141 | 144.6 | 492.4 | 1.984 | 140.0 | 53.91 |
| | 1 | 90.3 | 5.24 | 62.02 | 74 | 137 | 132.8 | 486.4 | 1.582 | 186.3 | 57.64 |
| | 3 | 102.6 | 5.43 | 66.05 | 75 | 136 | 127.0 | 479.2 | 1.423 | 254.3 | 59.52 |
| | 5 | 125.4 | 4.51 | 72.64 | 72 | 132 | 110.0 | 472.1 | 1.123 | 282.6 | 64.93 |
| FDMPO | 0.1 | 58.6 | 6.32 | 41.47 | 79 | 141 | 164.2 | 493.2 | 1.752 | 120.2 | 47.66 |
| | 1 | 87.2 | 5.37 | 60.67 | 78 | 133 | 154.6 | 488.4 | 1.651 | 160.3 | 50.72 |
| | 3 | 98.6 | 4.22 | 65.21 | 74 | 138 | 132.2 | 482.3 | 1.212 | 220.6 | 57.86 |
| | 5 | 120.2 | 3.89 | 71.46 | 75 | 136 | 116.0 | 478.6 | 1.134 | 260.4 | 63.02 |